3-1-1974

Design of Transmitter and Receiver Filters for Decision Feedback Equalization

Andres C. Salazar

THE BELL SYSTEM TECHNICAL JOURNAL
Vol. 53, No. 3, March 1974
Printed in U.S.A.

Design of Transmitter and Receiver Filters for Decision Feedback Equalization

By ANDRES C. SALAZAR

(Manuscript received August 14, 1973)

We present the constructive design of finite order equalizer filters for data transmission systems employing decision feedback equalization. Both transmitter design with power constraints and receiver design with ambient noise considerations are treated. Expressions for the filter tap settings which maximize a signal-to-noise ratio are found for both baseband pulse amplitude modulation and quadrature amplitude modulation (QAM) systems. Design examples are given in a passband equivalent (of QAM) formulation for an average toll telephone connection. Neglecting the possibility of error propagation, these examples demonstrate that decision feedback equalization requires fewer taps for acceptable system performance as compared to linear equalization. The problem of postcursor size in a decision feedback equalized response is treated and shown to diminish in importance when a hybrid equalization procedure is imposed on the linear tap adjustment. The price one pays for allowing the linear filter taps to reduce the postcursor sizes in this hybrid equalizer is a lower signal-to-noise ratio.

I. INTRODUCTION

The advantage of using a nonlinear device, referred to as a decision feedback equalizer, to cancel the tails of pulses whose amplitudes have already been estimated in a PAM system has long been recognized. Figure 1 depicts the typical system in which the decision feedback mechanism has always been envisioned to perform this task. Namely, by making decisions on a symbol-by-symbol basis and by knowing the channel response precisely, a data system would be designed so that postcursor (tails of preceding pulses) ISI could be eliminated without the ambient noise penalty that a linear filter or equalizer imposes. The tacit assumption being made in any decision feedback implementation is that the signal-to-noise ratio is high without

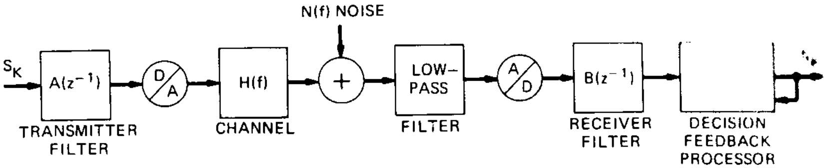

Fig. 1—Transmitter and receiver filter design.

equalization, and correct decisions are already being made with high probability.

In this paper we consider the design of finite order nonrecursive transmitting and receiving filters which counteract the two remaining sources of noise, the precursor tails which are the interfering samples of pulses whose amplitudes have not been decided upon, and ambient noise, everpresent in a communication system. In addition we seek the variation of the signal-to-noise ratio at the moment of decision when the sampling time is varied. Along with this variation of the criterion of system performance, we are also interested at each sampling time in the amount of postcursor ISI noise which the decision feedback mechanism is being asked to eliminate. This aspect of our investigation yields insight into the feasibility of decision feedback system implementation. It is, of course, possible to design the transmitting and receiving filters to achieve "hybrid" equalization between simple linear equalization and decision feedback. That is, some of the linear filter's degrees of freedom will be used to combat some postcursor ISI, although decision feedback is being used. The idea is to reduce the possibility that large postcursor tails will be produced by a linear filter whose sole job would otherwise be to reduce precursor ISI.

The system model we choose to work with is a sampled data or discrete one. In addition, the channel and the system's transmitting and receiving filters are assumed to be of finite nonrecursive type. Examples are discussed in a later section which involve voice-grade toll telephone channel spectra. These spectra have been reduced to a specified Nyquist equivalent bandwidth, both for baseband and passband applications. The timing involved in going from continuous waveforms to sampled data for these examples has been chosen to maximize a signal-to-noise criterion before any filtering is done at the receiver. Also, in the demodulation process for QAM, the carrier phase angle, if fixed, can be absorbed by the receiver's passband filter taps. (For more detail on the system model we use in the following sections, see Appendixes A and B.)

This paper follows two previous documents[1,2] that have dealt with asymptotic performance results concerning decision feedback equalization. In these previous works, the filters assumed in the decision feedback equalization scheme were of infinite length. In contrast, we focus our attention here on designing filters of finite, implementable length and study a channel which is modeled from transmission data taken from the 1969–70 Toll Connection Survey of the Bell System.

II. TRANSMITTER AND RECEIVER FILTER DESIGN (BASEBAND)

We begin by referring to Fig. 1 and denoting the channel response† by $\{h_n\}_0^M$. We are seeking nonrecursive filter tap weights $\{a_n\}_0^N$ and $\{b_n\}_0^N$, $N \ll M$ at the transmitter and receiver, respectively. We note the total response through the system is then

$$\{r_n\}_0^{M+2N+1} = \{a_n\}_0^N * \{h_n\}_0^M * \{b_n\}_0^N. \tag{1}$$

where $*$ denotes sequence convolution.

If we decide to sample at time τ and cancel‡ r_k, $k > \tau$ through decision feedback, then we can define a signal-to-noise ratio

$$\rho(N, \tau, \mathbf{a}, \mathbf{b}) \triangleq \frac{r_\tau^2}{\sigma^2\|\mathbf{b}\|^2 + \sum_{k<\tau} r_k^2} \tag{2}$$

representing the sampled signal in the numerator and two noise terms in the denominator. The first noise term consists of the ambient noise which is modified by the receiving filter. [We write $\mathbf{b}$ for $(b_0, b_1, \cdots, b_n)$ in E^{N+1} Euclidean space with $(\mathbf{a}, \mathbf{b})$ as the usual inner product and $\|\mathbf{b}\|^2 = (\mathbf{b}, \mathbf{b})$ the usual norm.] We have assumed that the noise samples are independent and of generalized variance§ σ^2 and that the input binary stream of symbols is independently and fairly signed and of unit magnitude. The second denominator term is a measure of the precursor ISI.

2.1 Filter design by integral adjustment

If we assume that the transmitter filter is to be optimized independently from the receiver filter we are then concerned with the

† Appendix A explains our use of the sampled response $\{h_n\}$. We suppress the constant multiplier $1/T$ which converts the z^{-1} coefficients to time samples (where T is the time between samples).

‡ We choose to cancel all postcursors. In practice, only a few are cancelled and others then become part of ISI term in (2).

§ By generalized variance we imply that a constant multiplies the true noise sample variance. This constant takes into account the sampling speed at which we are measuring the signal-to-noise ratio.

response:

$$\{g_n\}_0^{M+N} = \{a_n\}_0^N * \{h_n\}_0^M. \tag{3}$$

Define $\mathbf{a} = (a_0, a_1, \cdots, a_N)$ and $\mathbf{h}_k = (h_k, h_{k-1}, \cdots, h_{k-N})$. We seek the maximum of

$$\rho(N, \tau, \mathbf{a}) = \frac{(\mathbf{h}_\tau, \mathbf{a})^2}{\sigma^2 + \sum_{k<\tau} (\mathbf{h}_k, \mathbf{a})^2} \tag{4}$$

subject to the constraint that $\|\mathbf{a}\|^2 = \mu^2$. That is, we place an average power constraint on the transmitter. Hence, by constructing the quadratic form induced[3] by the sum of bilinear forms $(\mathbf{h}_k, \mathbf{a})^2$, we reshape $\rho(N, \tau, \mathbf{a})$ into

$$\rho(N, \tau, \mathbf{a}) = \frac{(\mathbf{h}_\tau, \mathbf{a})^2}{\mu^{-2}(\mathbf{a}, \sigma^2 I\mathbf{a}) + (\mathbf{a}, Q\mathbf{a})}, \tag{5}$$

where I is the $(N+1) \times (N+1)$ identity matrix and Q is the $(N+1) \times (N+1)$ positive semidefinite matrix $(\sum_{k<\tau} h_{k-i}h_{k-j})$ $0 \leqq i, j \leqq N$ with $h_{-l} \equiv 0$, $l > 0$. By use of the Cauchy-Schwartz inequality we find readily that the maximum of $\rho(N,\tau,\mathbf{a})$ is achieved at

$$\mathbf{a}^* = \frac{\mu[\mu^{-2}\sigma^2 I + Q]^{-1}\mathbf{h}_\tau}{\|[\mu^{-2}\sigma^2 I + Q]^{-1}\mathbf{h}_\tau\|} \tag{6}$$

and the maximum is precisely

$$\max_{\|\mathbf{a}\|^2=\mu^2} \rho(N, \tau, \mathbf{a}) = \rho(N, \tau, \mathbf{a}^*) = (\mathbf{h}_\tau, (\mu^{-2}\sigma^2 I + Q)^{-1}\mathbf{h}_\tau). \tag{7}$$

We note that the sequence $(h_0, h_1, \cdots, h_\tau)$ is mapped by the vector $\mathbf{a}^*$ into a sequence $(g_0^*, g_1^*, \cdots, g_\tau^*)$ which the receiver is now expected to process in forming the following signal-to-noise ratio:

$$\rho(N, \tau, \mathbf{a}^*, \mathbf{b}) = \frac{(\mathbf{g}_\tau^*, \mathbf{b})}{\sigma^2\|\mathbf{b}\| + \sum_{k<\tau} (\mathbf{g}_k^*, \mathbf{b})^2}, \tag{8}$$

where

$$\mathbf{g}_k^* = (g_k^*, g_{k-1}^*, \cdots, g_{k-N}^*).$$

Since $\rho(N, \tau, \mathbf{a}^*, \mathbf{b})$ is invariant to any scaling of $\mathbf{b}$, we choose to maximize the former with respect to $\|\mathbf{b}\| = 1$. By the same argument which led us to (6) and (7), we find

$$b^* = \frac{[\sigma^2 I + R]^{-1}\mathbf{g}_\tau^*}{\|[\sigma^2 I + R]^{-1}\mathbf{g}_\tau^*\|} \tag{9}$$

and

$$\rho(N, \tau, \mathbf{a}^*, \mathbf{b}^*) = \frac{1}{\|[\sigma^2 I + R]^{-1}\mathbf{g}_\tau^*\|}(\mathbf{g}_\tau^*, [\sigma^2 I + R]^{-1}\mathbf{g}_\tau^*), \tag{10}$$

where R is the $(N + 1) \times (N + 1)$ matrix $(\sum_{k<\tau} g_{k-i}^* g_{k-j}^*)$, $0 \leqq i$, $j \leqq N$. Hence, $\rho(N, \tau, \mathbf{a}^*, \mathbf{b}^*)$ in (10) represents the maximum signal-to-noise ratio achievable through the integral or independent adjustment of transmitter and receiver filters for a decision feedback system committed to sampling at time τ and constrained to use nonrecursive linear filters of length $N + 1$.

The difference between linear equalization and decision feedback can be seen readily by observing the denominator terms of the following signal-to-noise ratio:

$$\rho(N, \tau, \mathbf{a}, \mathbf{b}) = \frac{(\mathbf{g}_\tau, \mathbf{b})^2}{\sigma^2\|\mathbf{b}\|^2 + \sum_{k<\tau} (\mathbf{g}_k, \mathbf{b})^2 + \sum_{k>\tau} (\mathbf{g}_k, \mathbf{b})^2}. \tag{11}$$

For decision feedback systems, the last term in the denominator does not enter the picture because it is assumed it will be eliminated without noise penalty. However, in linear equalization, the filter $\mathbf{b}$ is expected not only to combat precursor ISI but postcursor ISI as well, with as little compromise to ambient noise as possible. We can rewrite (11) by assuming $\|\mathbf{b}\|^2 = 1$ (i.e., scaling irrelevant)

$$\rho(N, \tau, \mathbf{a}, \mathbf{b}) = \frac{(\mathbf{g}_\tau, \mathbf{b})^2}{[(\sigma^2 I + R_1 + R_2)\mathbf{b}, \mathbf{b}]}, \tag{12}$$

where R_1 and R_2 are, as usual, positive semidefinite channel response autocorrelation matrices. Here R_1 corresponds to precursor distortion while R_2 relates to postcursor ISI. We notice that, if we form for $0 \leqq \alpha \leqq 1$

$$\rho_\alpha(N, \tau, \mathbf{a}, \mathbf{b}) = \frac{(\mathbf{g}_\tau, \mathbf{b})^2}{[(\sigma^2 I + R_1 + \alpha R_2)\mathbf{b}, \mathbf{b}]}, \tag{13}$$

we can continuously vary $\rho_\alpha(N, \tau, \mathbf{a}, \mathbf{b})$ from the decision feedback formulation where $\alpha \equiv 0$ to the linear equalization case where $\alpha \equiv 1$. Thus, although we implement decision feedback equalization, it is possible to design the transmitting and receiving filters so that the amount of postcursor distortion is still mildly to strongly influential. Of course, a more general formulation of this "hybrid" design technique is possible by retracing our steps back to (11) and forming

$$\rho(N, \tau, \mathbf{a}, \mathbf{b}) = \frac{(\mathbf{g}_\tau, \mathbf{b})^2}{\sigma^2\|\mathbf{b}\|^2 + \sum_{k<\tau} (A_k \mathbf{g}_k, \mathbf{b})^2 + \sum_{k>\tau} (A_k \mathbf{g}_k, \mathbf{b})^2}, \tag{14}$$

where A_k are $(N+1) \times (N+1)$ diagonal matrices (obviously $A_k \equiv I$ for the linear equalizer case).[†]

2.2 Joint optimization of transmitter and filter design (baseband)

In the individual design of transmitter and receiver filters treated in the last section, we were able to find the optimal filters by a simple rearrangement of interference terms and applying the Cauchy-Schwartz inequality. We find that for joint filter optimization this procedure will be slightly modified and additional steps will be taken to arrive at the solution.

We recall that the total response of the system depicted in Fig. 1 is

$$\{r_n\}_0^{M+2N} = \{a_n\}_0^N * \{h_n\}_0^M * \{b_n\}_0^N \tag{15}$$

and the signal-to-noise ratio:

$$\rho(N, \tau, \mathbf{a}, \mathbf{b}) = \frac{(\mathbf{c}, \mathbf{h}_\tau)^2}{\sigma^2\|\mathbf{b}\|^2 + \sum\limits_{k<\tau} (\mathbf{c}, \mathbf{h}_k)^2}, \tag{16}$$

where $\mathbf{c}$ is the $2N+1$ dimensional vector formed from the sequence $\{a_n\}_0^N * \{b_n\}_0^N$ and $\mathbf{h}_k = (h_k, h_{k-1}, \cdots, h_{k-2N})$. Here again, $\rho(N, \tau, \mathbf{a}, \mathbf{b})$ is seen to be a continuous function of $\mathbf{a}$ and $\mathbf{b}$ and functionally invariant to the norm of $\mathbf{b}$. Hence, we constrain our search for the optimal $\mathbf{b}$ vector by imposing $\|\mathbf{b}\| = 1$.

The transmitter power constraint was imposed in Section 2.1 by $\|\mathbf{a}\| = \mu^2$. In practical situations, the constraint is more likely to be $\|\mathbf{a}\| \leqq \mu^2$. That is, we want to use only enough power to yield a sufficiently high signal-to-noise ratio at the receiver. For example, we constrain the receiver filter to be of unit norm since the norm is not going to contribute toward the enhancement of the signal-to-noise ratio at its output. Rather, it will be the transmitter filter power output which determines the output signal-to-noise ratio to a large extent. A way of solving the joint filter optimization problem with constraints, then, is by permitting the transmitter power level to be at that as-yet undetermined level so that the signal power through the transmitter, channel, and receiver will be at a prespecified ratio to that of the ambient noise. Hence, we have the following optimization problem:

$$\max_{\substack{\|\mathbf{h}*\mathbf{a}*\mathbf{b}\| = \eta \\ \|\mathbf{b}\| = 1}} \rho(N, \tau, \mathbf{a}, \mathbf{b}) = \max_{\substack{\|\mathbf{h}*\mathbf{a}*\mathbf{b}\| = \eta \\ \|\mathbf{b}\| = 1}} \frac{(\mathbf{a}*\mathbf{b}, \mathbf{h}_\tau)^2}{\sigma^2 + \sum\limits_{k<\tau} (\mathbf{a}*\mathbf{b}, \mathbf{h}_k)^2}. \tag{17}$$

[†] Of course, some constraint must be put on A_k to make the maximization of ρ meaningful.

Proceeding as before, we obtain

$$(\mathbf{a}*\mathbf{b})^* = k_0\left(\frac{\sigma^2}{\eta^2}H^TH + R\right)^{-1}\mathbf{h}_\tau, \tag{18}$$

(where k_0 is determined from the constraint $\|\mathbf{h}*\mathbf{a}*\mathbf{b}\| = \eta$) with

$$\rho(N, \tau, \mathbf{a}^*, \mathbf{b}^*) = \left(\mathbf{h}_\tau, \left(\frac{\sigma^2}{\eta^2}H^TH + R\right)^{-1}\mathbf{h}_\tau\right), \tag{19}$$

where H is the $2M + 1 \times 2N + 1$ matrix such that $H(\mathbf{a}*\mathbf{b}) = \mathbf{h}*\mathbf{a}*\mathbf{b}$ where $\mathbf{h} = (h_0, h_1, h_2, \cdots, h_M)$. The matrix R is formed from the $\sum_{k<\tau} h_{k-i}h_{k-j}$ terms. Now (18) can be written in its z^{-1} transfer function representation.

$$\begin{aligned}(\mathbf{a}*\mathbf{b})^*(z^{-1}) &= k(1 + \alpha_1 z^{-1} + \alpha_2 z^{-2} + \cdots + \alpha_{2N} z^{-2N}) \\ A(z^{-1})B(z^{-1}) &= kQ_1(z^{-1})Q_2(z^{-1})\cdots Q_N(z^{-1}),\end{aligned} \tag{20}$$

where k is a determined constant and the Q's are quadratic factors with real coefficients. A choice of the quadratic factors for composing $A(z^{-1})$ and $B(z^{-1})$ exists. However, since $\|\mathbf{b}^*\| = 1$ we are then left with a determinable norm for $\mathbf{a}^*$. For example, we might choose

$$B^*(z) = \frac{Q_1(z^{-1})}{\|Q_1(z^{-1})\|}. \tag{21}$$

Hence,

$$A^*(z^{-1}) = \|Q_1(z^{-1})\|\cdot kQ_2(z^{-1})\cdots Q_n(z^{-1}), \tag{22}$$

with norm

$$\|A^*(z^{-1})\| = k\|Q_1(z^{-1})\|\|Q_2(z^{-1})\cdots Q_n(z^{-1})\|.$$

Regardless of how the quadratic factors are assigned, $B^*(z^{-1})$ is normalized and $A^*(z^{-1})$ is then left with some norm value which may be large or small. The total norm $\|\mathbf{a}*\mathbf{h}*\mathbf{b}\|$, however, was chosen to be η and for each receiver filter chosen from the quadratic factors of (20), a corresponding $\|A^*(z^{-1})\|$ results. It is of definite engineering interest to seek that quadratic factor combination which minimizes $\|A^*(z^{-1})\|$, but no obvious solution exists for this combinatorial problem. Other considerations may come into play at this point which would obviate the need for minimizing $\|A^*(z^{-1})\|$. For example, a minimum phase requirement for one of the two filters would delineate the two filters. Roundoff noise considerations for digital filter implementations might also contribute toward selecting one quadratic factor over another at the receiver. Cost considerations may warrant the splitting of the two filters into equal lengths (N even) so that the number of possible quadratic combinations is reduced considerably. In any case, this filter-splitting problem is akin to the quadratic factor placement problem in minimizing roundoff noise in digital filter implementations. In Appendix D we outline a technique for separating the transmitter and receiver filters.

Of course, it is possible to go through the same generalization on postcursor and precursor equalization that we did for the integral optimization problems of Section II. We obtain in that case

$$\rho(N, \tau, \mathbf{a}^*, \mathbf{b}^*) = \left[\mathbf{h}_\tau, \left(\frac{\sigma^2}{\eta^2} H^T H + R_1 + \alpha R_2\right)^{-1} \mathbf{h}_\tau\right], \tag{23}$$

where

$$\mathbf{a}*\mathbf{b} = k_0 \left(\frac{\sigma^2}{\eta^2} H^T H + R_1 + \alpha R_2\right)^{-1} \mathbf{h}_\tau \tag{24}$$

and where $R_1(R_2)$ is the matrix corresponding to precursor (postcursor) interference terms and $0 \leqq \alpha \leqq 1$.

III. PASSBAND FORMULATION

It is possible to extend the results outlined in the previous sections to the passband equivalents of transmitter, channel, and receiver for a quadrature amplitude modulation (QAM) system.† The extension of results is not without complications, since QAM systems suffer from another form of distortion—co-channel interference (CCI). Thus, the transmitting and receiving filters will be expected to combat not only ambient noise and ISI but also co-channel intersymbol interference (CCISI).

3.1 *Integral optimization*

We begin by referring to Fig. 2 which illustrates the QAM system with decision feedback. We are interested in the transmitter and receiver filter designs so that a measure of transmission performance is maximized. Namely, we seek to maximize a sampled signal-to-generalized-noise ratio similar to that defined in (2). To define the terms which will appear in our performance measure, we note that the "in-phase" response at the receiver is

$$\begin{aligned}\{r_k^{(p)}\}_0^{M+2N} = {} & \{a_k^{(p)}\}_0^N * [\{h_k^{(p)}\}_0^M * \{b_k^{(p)}\}_0^N - \{h_k^{(q)}\}^M * \{b_k^{(q)}\}_0^N] \\ & - \{a_k^{(q)}\}_0^N * [\{h_k^{(q)}\}_0^M * \{b_k^{(p)}\}_0^N + \{h_k^{(p)}\}_0^M \{b_k^{(q)}\}_0^N],\end{aligned} \tag{25}$$

while the "quadrature" response at the receiver is

$$\begin{aligned}\{r_k^{(q)}\}_0^{M+2N} = {} & \{a_k^{(p)}\}_0^N * [\{h_k^{(p)}\}_0^M * \{b_k^{(q)}\}_0^N + \{h_k^{(q)}\}_0^M * \{b_k^{(p)}\}_0^N] \\ & + \{a_k^{(q)}\}_0^N * [\{h_k^{(p)}\}_0^M * \{b_k^{(p)}\}_0^N - \{h_k^{(q)}\}_0^M * \{b_k^{(q)}\}_0^N].\end{aligned} \tag{26}$$

† We will not concern ourselves with the problems of carrier acquisition and timing for the QAM system we consider here in discrete form (see Appendix A for a discussion of these items).

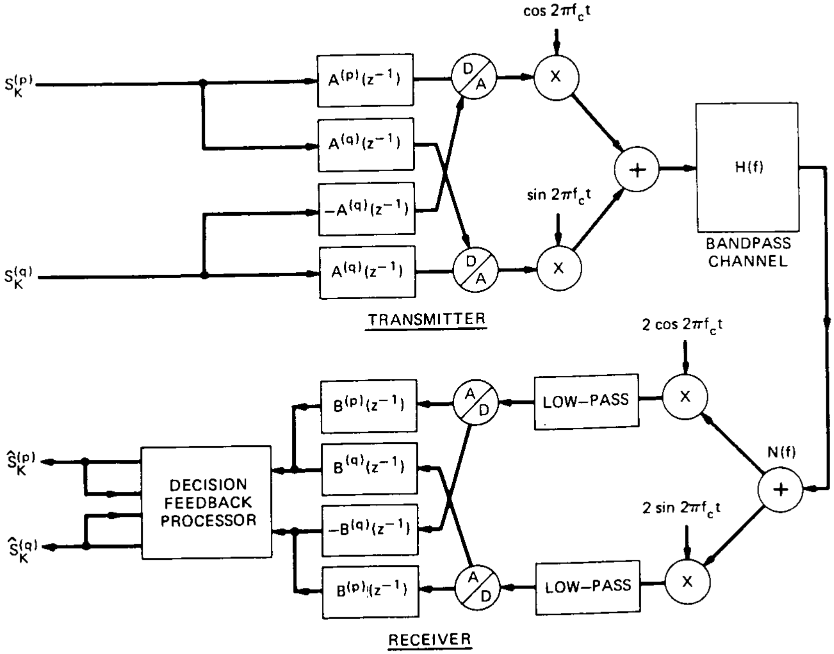

Fig. 2—QAM data system with decision feedback equalization.

Each channel response has two ISI components, an in-channel intersymbol interference term and the other due to co-channel interference. We notice that the CCI is completely eliminated if $\{b_k^{(p)}\} \equiv \{h_k^{(q)}\}$ and $\{b_k^{(q)}\} \equiv \{h_k^{(p)}\}$. However, in our considerations we will always assume $M \gg N$ so that our filters do not have a sufficient number of degrees of freedom to eliminate CCI (also, this action does constitute suboptimal filtering).

We form the in-phase resultant signal-to-noise ratio for independent input channels, independent symbols of unit magnitude with equal chance of occurrence and uncorrelated noise samples of variance σ^2. We first treat the case where the receiver filter is all pass (i.e., $\mathbf{b} = \mathbf{e}$, the identity vector in the algebra of convolution)

$$\rho_s(\underset{\mathbf{b}=\mathbf{e}}{N}, \tau, \mathbf{a}, \mathbf{b}) = \frac{[(\mathbf{a}^{(p)}, \mathbf{h}_\tau^{(p)}) - (\mathbf{a}^{(q)}, \mathbf{h}_\tau^{(q)})]^2}{\sigma^2 + \sum_{k<\tau} [(\mathbf{a}^{(p)}, \mathbf{h}_k^{(p)}) - (\mathbf{a}^{(q)}, \mathbf{h}_k^{(q)})]^2 + \cdots + \sum_{k \leq \tau} [(\mathbf{a}^{(q)}, \mathbf{h}_k^{(p)}) + (\mathbf{a}^{(p)}, \mathbf{h}_k^{(q)})]^2}. \quad (27)$$

Now we define

$$\mathbf{a} = [\mathbf{a}^{(p)}, \mathbf{a}^{(q)}]$$

and $\mathbf{h}_\tau = [\mathbf{h}_\tau^{(p)}, -\mathbf{h}_\tau^{(q)}]$ and $\mathbf{h}_\tau^R = [\mathbf{h}_\tau^{(q)}, \mathbf{h}_\tau^{(p)}]$, vectors of $2N + 2$ unit length. Hence, we can rewrite (27) into

$$\rho_s(\underset{\mathbf{b}=\mathbf{e}}{N, \tau, \mathbf{a}, \mathbf{b}}) = \frac{(\mathbf{a}, \mathbf{h}_\tau)^2}{\sigma^2 + \sum_{k<\tau} (\mathbf{a}, \mathbf{h}_k)^2 + \sum_{k \leqq \tau} (\mathbf{a}, \mathbf{h}_k^R)^2}. \tag{28}$$

In (27) and (28) we have tacitly assumed that at the receiver each channel will "talk" to the other for the purpose of cancelling postcursor CCISI also.† That is, we have assumed a dual system of decision feedback equalization is being implemented.

The maximization of $\rho_s(N, \tau, \mathbf{a}, \mathbf{b})$ subject to $\mathbf{b} = \mathbf{e}$ and $\|\mathbf{a}\|^2 = \mu^2$ leads to a solution similar to that of (6) and (7):

$$\mathbf{a}^* = \frac{\mu[\mu^{-2}\sigma^2 I + Q + Q_c]^{-1}\mathbf{h}_\tau}{\|[\mu^{-2}\sigma^2 I + Q + Q_c]^{-1}\mathbf{h}_\tau\|} \tag{29}$$

$$\max_{\substack{\|\mathbf{a}\|^2=\mu^2 \\ \mathbf{b}=\mathbf{e}}} \rho(N, \tau, \mathbf{a}, \mathbf{b}) = \rho(N, \tau, \mathbf{a}^*, \mathbf{e})$$

$$= \frac{\mu(\mathbf{h}_\tau, (\mu^{-2}\sigma^2 I + Q + Q_c)^{-1}\mathbf{h}_\tau)}{\|[\mu^{-2}\sigma^2 I + Q + Q_c]^{-1}\mathbf{h}_\tau\|}, \tag{30}$$

where Q and Q_c are respectively the in-phase and co-channel correlation matrices similarly formed, as was the Q matrix of (6). The $\mathbf{a}^*$ vector of (29) separates into $\mathbf{a}^{*(p)}$ and $\mathbf{a}^{*(q)}$ and the conditionally optimal transmitter bandpass filter is completely specified. Following the procedure in Section II, we now hold the transmitter design fixed at $\mathbf{a}^*$ and rewrite (25) as

$$\begin{aligned}\{r_k^{(p)}\}_0^{M+2N}|_{\mathbf{a}=\mathbf{a}^*} = {} & \{b_k^{(p)}\}_0^N * \{\{a_k^{*(p)}\}_0^N * \{h_k^{(p)}\}_0^M\} \\ & - \{b_k^{(q)}\}_0^N * \{\{a_k^{*(p)}\}_0^N * \{h_k^{(q)}\}_0^M\} \\ & - \{b_k^{(q)}\}_0^N * \{\{a_k^{*(q)}\}_0^N * \{h_k^{(p)}\}_0^M\} \\ & - \{b_k^{(p)}\}_0^N * \{\{a_k^{*(q)}\}_0^N * \{h_k^{(q)}\}_0^M\} \end{aligned} \tag{31}$$

$$\begin{aligned} = {} & \{b_k^{(p)}\}_0^N * \{\{g_k^{(pp)}\}_0^{M+N} - \{g_k^{(qq)}\}_0^{M+N}\} \\ & - \{b_k^{(q)}\}_0^N * \{\{g_k^{(qp)}\}_0^{M+N} + \{g_k^{(pq)}\}_0^{M+N}\}, \end{aligned} \tag{32}$$

where $\{g_k^{(u)}\}_0^{M+N}$, $u = pp, pq, qp, qq$ are recognizable from (31).

We can now write the expression for $\rho(N, \tau, \mathbf{a}^*, \mathbf{b})$ as

$$\rho(N, \tau, \mathbf{a}^*, \mathbf{b}) = \frac{[(\mathbf{b}^{(p)}, \mathbf{g}_\tau^{(p)}) - (\mathbf{b}^{(q)}, \mathbf{g}_\tau^{(q)})]^2}{\sigma^2\|\mathbf{b}\|^2 + \sum_{k<\tau} [(\mathbf{b}^{(p)}, \mathbf{g}_k^{(p)}) - (\mathbf{b}^{(q)}, \mathbf{g}_k^{(q)})]^2 + \cdots}$$
$$+ \sum_{k \leqq \tau} [(\mathbf{b}^{(q)}, \mathbf{g}_k^{(p)}) + (\mathbf{b}^{(p)}, \mathbf{g}_k^{(q)})]^2, \tag{33}$$

† Also, we are assuming we will eliminate all postcursor ISI. However, in practice, only a few postcursors would be removed. Thus, some postcursor terms would appear in the denominator of (28) in that case.

where

$$\mathbf{g}_\tau^{(p)} = (g_\tau^{(pp)} - g_\tau^{(qq)}, g_{\tau-1}^{(pp)} - g_{\tau-1}^{(qq)}, \cdots, g_{\tau-N}^{(pp)} - g_{\tau-N}^{(qq)}), \tag{34}$$

and similarly for $\mathbf{g}_\tau^{(q)}$. To maximize $\rho(N, \tau, \mathbf{a}^*, \mathbf{b})$ subject to $\|\mathbf{b}\| = 1$, we first form the concatenated vectors of $2N + 2$ length:

$$\mathbf{b} = (\mathbf{b}^p, \mathbf{b}^q), \quad \mathbf{g}_k = (\mathbf{g}_k^{(p)}, -\mathbf{g}_k^{(q)}), \quad \mathbf{g}_k^c = (\mathbf{g}_k^{(q)}, \mathbf{g}_k^{(p)}). \tag{35}$$

Hence

$$\rho(N, \tau, \mathbf{a}^*, \mathbf{b}) = \frac{(\mathbf{b}, \mathbf{g}_\tau)^2}{\sigma^2\|\mathbf{b}\|^2 + \sum_{k<\tau} (\mathbf{b}, \mathbf{g}_k)^2 + \sum_{k \leqq \tau} (\mathbf{b}, \mathbf{g}_k^c)^2}, \tag{36}$$

and we proceed to find that

$$\max_{\|\mathbf{b}\|=1} \rho(N, \tau, \mathbf{a}^*, \mathbf{b}) = [\mathbf{g}_\tau, (\sigma^2 I + R + R_c)^{-1}\mathbf{g}_\tau] \tag{37}$$

achieved at

$$\mathbf{b}^* = \frac{(\sigma^2 I + R + R_c)^{-1}\mathbf{g}_\tau}{\|(\sigma^2 I + R + R_c)^{-1}\mathbf{g}_\tau\|}, \tag{38}$$

where R and R_c are channel response correlation matrices of the type encountered before.

3.2 Joint optimization

To jointly optimize the transmitter and receiver passband filters, we follow virtually the same procedure found successful for the baseband case. A comparable factorization problem arises here, for which only a combinatorial solution seems to exist.

The in-phase and quadrature responses through a passband transmitter, channel, and receiver are given by

$$\begin{aligned}\{r_k^{(p)}\}_0^{M+2N} = \{h_k^{(p)}\}_0^M &* (\{a_k^{(p)}\}_0^N * \{b_k^{(p)}\}_0^N - \{a_k^{(q)}\}_0^N * \{b_k^{(q)}\}_0^N) \\ &- \{h_k^{(q)}\}_0^M * (\{a_k^{(p)}\}_0^N * \{b_k^{(q)}\}_0^N + \{a_k^{(q)}\}_0^N * \{b_k^{(p)}\}_0^N)\end{aligned} \tag{39}$$

$$\begin{aligned}\{r_k^{(q)}\}_0^{M+2N} = \{h_k^{(p)}\}_0^M &(\{a^{(p)}\}_0^N * \{b^{(q)}\}_0^N + \{a^{(q)}\}_0^N * \{b_0^{(p)}\}_0^N) \\ &+ \{h_k^{(q)}\}_0^M * (\{a_k^{(p)}\}_0^N * \{b_k^{(p)}\}_0^N - \{a_k^{(q)}\}_0^N * \{b_k^{(q)}\}_0^N).\end{aligned} \tag{40}$$

Rewriting (39) and (40) in terms of a combined passband filter with responses $\mathbf{c}^{(p)} = \{c_k^{(p)}\}_0^{2N}$ and $\mathbf{c}^{(q)} = \{c_k^{(q)}\}_0^{2N}$:

$$\{r_k^{(p)}\}_0^{M+2N} = \{h_k^{(p)}\}_0^M * \{c_k^{(p)}\}_0^{2N} - \{h_k^{(q)}\}_0^M * \{c_k^{(q)}\}_0^{2N} \tag{41}$$

$$\{r_k^{(q)}\}_0^{M+2N} = \{h_k^{(p)}\}_0^M * \{c_k^{(q)}\}_0^{2N} + \{h_k^{(q)}\}_0^M * \{c_k^{(p)}\}_0^{2N}, \tag{42}$$

we form the augmented vectors $\mathbf{c} = [\mathbf{c}^{(q)}, \mathbf{c}^{(p)}]$,

$$\mathbf{h}_k = (h_k^{(p)}, h_{k-1}^{(p)}, \cdots, h_{k-2N}^{(p)}, -h_k^{(q)}, \cdots, -h_{k-2N}^{(q)})$$

and

$\mathbf{h}_k^R = (h_k^{(q)}, h_{k-1}^{(q)}, \cdots, h_{k-2N}^{(q)}, h_k^{(p)}, \cdots, h_{k-2N}^{(p)}), h_k^{(n)} = 0, k < 0, n = p,q.$

Our signal-to-noise ratio becomes for the in-phase channel:

$$\rho(N, \tau, \mathbf{c}) = \frac{(\mathbf{c}, \mathbf{h}_\tau)^2}{\sigma^2\|\mathbf{b}\|^2 + (R\mathbf{c}, \mathbf{c}) + (R_c\mathbf{c}, \mathbf{c})}, \tag{43}$$

where R and R_c are the now-familiar channel correlation matrices and $\mathbf{b} = (\mathbf{b}^{(p)}, \mathbf{b}^{(q)})$. It is easy to show that the norm of the receiver filter is irrelevant in the maximization of $\rho(N, \tau, \mathbf{c})$. Hence, we choose $\|\mathbf{b}\| = 1$. We now specify the amount of signal power η^2 we will need at the receiver upon choosing the optimal filters. That is,

$$\sum_{k=0}^{M+2N} |(\mathbf{h}_k, \mathbf{c})|^2 + |(\mathbf{h}_k^R, \mathbf{c})|^2 = \eta^2. \tag{44}$$

But (44) can be rewritten

$$\frac{(Q\mathbf{c}, \mathbf{c})}{\eta^2} = 1, \tag{45}$$

where Q is a sum of two correlation matrices. Hence, (43) then yields the problem:

$$\max_{\substack{\|\mathbf{b}\|=1 \\ (Q\mathbf{c},\mathbf{c})=\eta^2}} \frac{(\mathbf{c}, \mathbf{h}_\tau)^2}{\dfrac{\sigma^2(Q\mathbf{c}, \mathbf{c})}{\eta^2} + (R\mathbf{c}, \mathbf{c}) + (R_c\mathbf{c}, \mathbf{c})} \tag{46}$$

to which the solution is

$$\mathbf{c}^* = k\left(\frac{\sigma^2 Q}{\eta^2} + R + R_c\right)^{-1}\mathbf{h}_\tau \tag{47}$$

and

$$\rho(N, \tau, \mathbf{c}^*) = \left[\mathbf{h}_\tau, \left(\frac{\sigma^2 Q}{\eta^2} + R + R_c\right)^{-1}\mathbf{h}_\tau\right].$$

The constant k is determined from the constraint that $(Q\mathbf{c}, \mathbf{c}) = \eta^2$. Since $\mathbf{c} = (\mathbf{c}^{(q)}, \mathbf{c}^{(p)})$ and the vectors $(\mathbf{a}^{(p)}, \mathbf{a}^{(q)})$ and $(\mathbf{b}^{(p)}, \mathbf{b}^{(q)})$ all make up $\mathbf{c}^{(p)}$ and $\mathbf{c}^{(q)}$, we encounter a factorization problem. We can choose $(\mathbf{b}^{(p)}, \mathbf{b}^{(q)})$, normalize the receiver filter, and then are left with the transmitter filter which has a given norm. This norm is then the transmitter power required to produce η^2/σ^2 generalized signal-to-noise power at the receiver.

IV. EXAMPLES

To illustrate the difference in performance between decision feedback and linear equalization, we have taken a telephone DDD toll connection as a linear channel model. Specifically, we would like to know the difference in performance on a telephone connection when both linear and decision feedback equalization schemes are constrained to use a finite number of taps. For comparison, we compute the performance asymptotes (infinite number of taps) for each equalization scheme (see Appendix C) realized when an infinite number of taps are available. We ask whether it is possible to approach these asymptotes with a reasonable (implementable) number of taps. Another point which is raised in every implementation of decision feedback equalization is that of postcursor size. If a mistake in symbol identification is made, then the subtraction, for example, of an erroneously signed postcursor may lead to a burst of errors if the postcursor size is large. We illustrate the postcursor sizes for a passband decision feedback equalization system operating on an average telephone connection.

Figure 3 illustrates the magnitude characteristic of the average DDD toll telephone connection as measured in the 1969–70 Toll Connection Survey of the Bell System. The corresponding delay characteristic follows a parabolic shape and has been numerically integrated to yield a phase curve. As discussed in Appendix B, the bandpass channel parameters have been calculated for various carriers and various flat Nyquist spectral widths assumed at the transmitter. The spectral width was controlled by superimposing a cosine rolloff (400-Hz width centered at the Nyquist frequency) on the in-phase and quadrature spectra. Figures 4 and 5 show typical passband spectra computed for this channel. When this decomposition of the bandpass channel into in-phase and quadrature responses is achieved, it is possible to compute the performance asymptotes for linear and decision feedback equalization given in Appendix C. The result of these computations is shown in Table I. It is seen that performance decreases

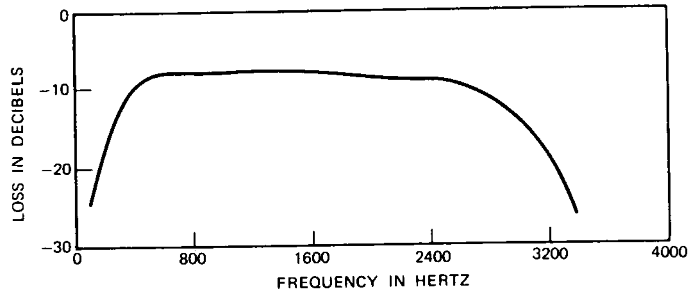

Fig. 3—Average amplitude characteristic for toll telephone connection (from 1969–70 Toll Connection Survey data).

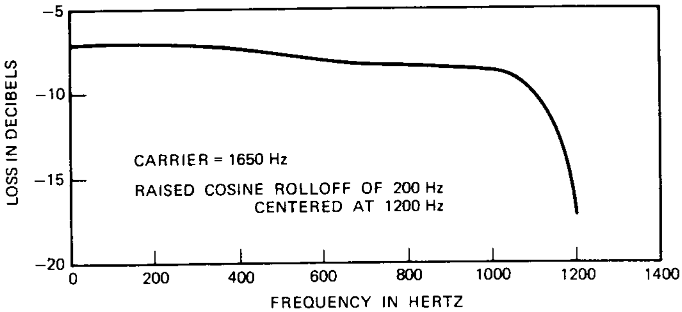

Fig. 4—Quadrature amplitude characteristic for average toll telephone connection.

with data rate and slightly with increased carrier frequency. The gap between decision feedback and linear equalization widens as speed is increased. For all computations, we have kept the total transmitted power through the channel fixed at -12 dBm, whereas the noise power spectral density was kept at that level corresponding to total noise power of -48.3 dBm over a 0–3000 Hz bandwidth. This noise level is 3 dB weaker† than the average noise power measured in the 1969–70 Toll Connection Survey.

A finite length receiving filter was increased in length until performance was reasonably close to the asymptote given in Table I for that speed and carrier. Figure 6 illustrates the difference in performance between decision feedback and linear equalization. It is seen that less than half the number of taps are required by the decision feedback

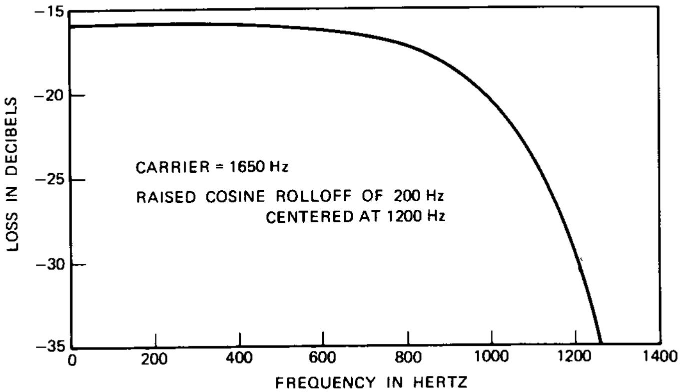

Fig. 5—In-phase amplitude characteristic for average toll telephone connection.

† Noise level was made weaker only for computational convenience.

Table I — QAM transmission asymptotic SNR in dB for average toll telephone connection
Noise at receiver — 48.3 dBm; transmitted power — 12 dBm

Rate in Baud/ch.	Carrier = 1650 Hz			Carrier = 1700 Hz			Carrier = 1800 Hz		
	L.E.	D.F.	M.F.	L.E.	D.F.	M.F.	L.E.	D.F.	M.F.
2400	31.4	31.9	32.1	30.7	31.6	31.9	29.2	30.9	31.6
2600	31.3	31.5	31.7	31.1	31.3	31.5	30.5	30.9	31.2
2800	27.3	30.4	31.1	28.5	30.2	30.9	28.8	29.9	30.5
3000	27.8	29.8	30.6	27.8	29.6	30.4	25.5	28.7	29.9
3200	25.5	29.0	30.1	25.1	28.6	29.9	19.4	27.4	29.4

L.E. = Linear equalization asymptote. D.F. = Decision feedback asymptote. M.F. = Matched filter bound.

equalizer to achieve a level of performance close to the asymptote. In addition, the linear equalizer even with its 36 tap length per channel could not keep an acceptable performance level when the data speed was increased to 3200 symbols/s/channel. On this basis, the premise that decision feedback equalization has significant advantages over linear equalization may be too readily accepted. For, if we examine postcursor sizes on one of these equalized bandpass channels, we can see that the high signal-to-noise ratio offered by decision feedback does not come without penalty. Figure 7 illustrates sample sizes of a toll telephone channel equalized with a 16-tap (8-feedback) decision feedback equalizer. The precursors, or samples before the main sample peak, are too small to be seen on this scale. However, it is clear that the postcursor adjacent to the signal sample, which is greater than half the latter's size, presents a problem. Should a decision error occur, the next signal sample could have its polarity reversed, since more than twice its strength could be subtracted out by the decision feedback processor. Thus, error propagation is possible with only a single mistake providing the ignition. Let us recall the hybrid equalization scheme discussed in Section II. We note in Fig. 8 that, for an alpha value of 0.01, we diminish the size of the large postcursor and more evenly distribute the heights of all the postcursors to be subtracted by the decision feedback processor. It is now apparent that no one postcursor is large enough to reverse the polarity of the signal should a decision error occur. It will take several consecutive decision errors, for example, before this can happen now. However, we lose 1 dB in signal-to-noise ratio for this example when we opt for this mitigation of the postcursor size problem. Of course, a trade-off exists between

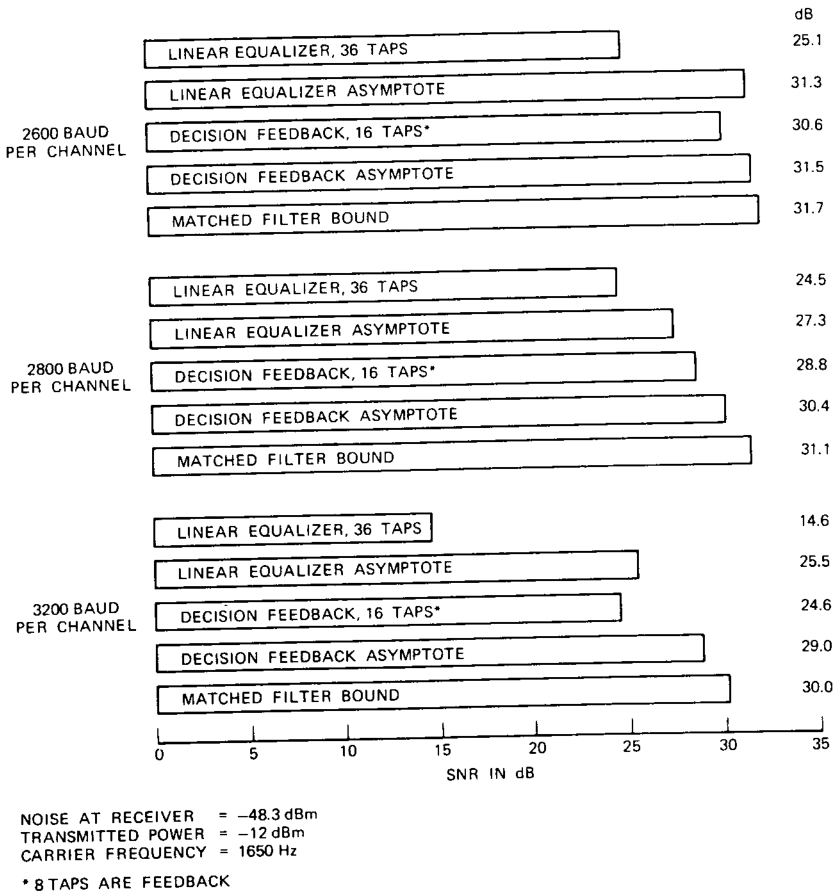

Fig. 6—Performance of finite equalizers for average toll telephone connection.

the loss in signal-to-noise ratio and reduction of postcursor size by means of this method.

V. SUMMARY

We have treated the design of finite length transmitting and receiving filters for a data system employing decision feedback equalization. Our purpose here was to examine the difference in performance between linear and decision feedback equalization on a given data channel. Sequential and joint optimization of transmitting and receiving filters were treated for an all-Nyquist equivalent data system. Although the solutions for the optimum tap settings

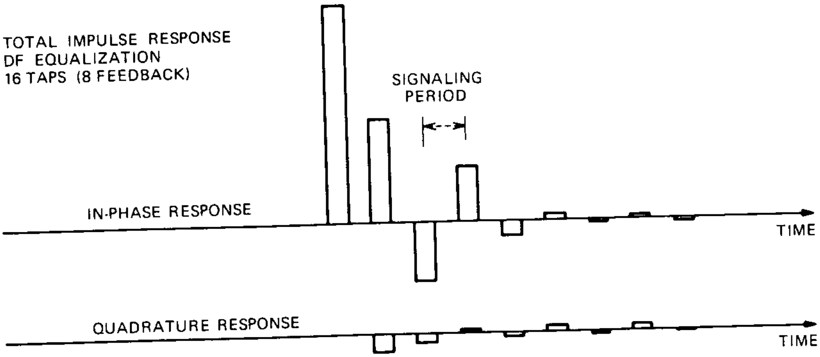

Fig. 7—Postcursor size problem and mitigation.

and signal-to-noise ratio were derived in general terms, applying the results to the spectrum of a toll telephone connection was of special interest. For this channel example, it was found that fewer filter taps were required for decision feedback equalization to achieve a reasonable performance level. The problem of postcursor size for an overall response of a passband decision feedback equalized system can be mitigated by a hybrid equalization scheme. The price for allowing the linear filter taps to diminish the postcursor sizes in this hybrid equalizer is a lower signal-to-noise ratio.

APPENDIX A

Details about the discrete channel model

The lowpass filters in the A/D or D/A conversion process shown in Figs. 1 and 2 delimit the channel frequency band which supports data

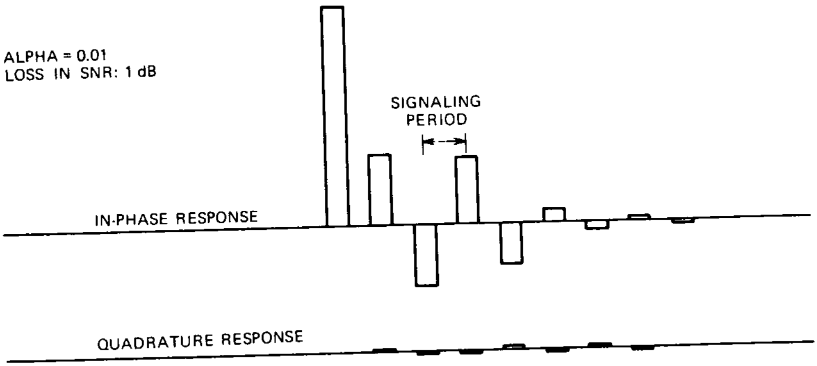

Fig. 8—Total impulse response hybrid equalization.

transmission. Hence, the channel can be seen as a bandlimited medium and can also be reduced to discrete form for M sufficiently large:

$$H(f) = \sum_{n=0}^{M} \equiv h_n \, e^{-jn2\pi fT} \quad |f| \leqq \frac{T}{2},$$

where T is the data symbol interval or $1/2T$ is the Nyquist frequency. The point here is that $\{h_n\}$ is dependent on the timing chosen for this reduction. Obviously, a timing exists which maximizes a signal-to-noise ratio, for example, of the unequalized response. We have found by experimentation that this timing was an excellent approximation to the timing which leads to a maximum signal-to-noise ratio after equalization.

For a bandpass channel, the decomposition into discrete form takes place in two steps. First, a carrier frequency is chosen, and in-phase and quadrature spectra are then computed. A constant carrier phase is then a variable parameter. However, it is easily shown that this carrier constant can be absorbed by either the demodulation process or the passband equalizer tap settings.

It is important to recall that the time samples of the spectrum

$$H(f) = \sum_{n=0}^{M} h_n \, e^{-jn2\pi fT}$$

are $\{\frac{1}{T} \cdot h_n\}_0^M$. Hence, in the formation of the signal-to-noise ratio:

$$\rho = \frac{h_\tau^2}{\sigma^2 T^2 + \text{ISI}}$$

we form the generalized variance parameter $\sigma^2 T^2$ where σ^2 is the noise sample variance. This accounts for this transformation from Fourier coefficients $\{h_n\}_0^M$ to time samples $\{1/T \cdot h_n\}_0^M$.

APPENDIX B

Channel data from 1969–70 toll connection survey

The average loss and delay measurements of over 600 toll voice-grade connections made in a 1969–70 survey are recorded in Ref. 4. For our channel model, interpolative curves were constructed from the average survey measurements made on 20 frequencies. A linear loss slope was appended at the lower frequency end to extrapolate loss down to zero frequency. The slope of the loss curve in decibels at the lowest measurement frequency (200 Hz) was used for this extrapolation. A constant was added to the integrated delay curve to achieve zero phase at zero frequency.

Passband responses at several carrier frequencies were then formulated from the interpolated baseband data. An impulse response was calculated for each in-phase and quadrature channel. Timing for the two channels was chosen to maximize the squared sampled signal to mean square ISI and CCISI before the receiver filter. One hundred eight Nyquist samples ($\{h_n^{(p)}\}_{h=0}^{179}$ and $\{h_n^{(q)}\}_0^{179}$) represented each passband channel.

APPENDIX C

Asymptotic MSE as derived by Falconer-Foschini[2]

We list here the formulas for the MSE as achieved by linear equalization and decision feedback for passband systems (here, independent binary ± 1 transmission is assumed with $N_0/2$ input noise spectrum).

$$(\text{MMSE})_{\text{linear}} = \int_{-1/2T}^{1/2T} T\left(\frac{X_0(f)}{N_0} + 1\right)^{-1} \text{df} \tag{48}$$

$$(\text{MMSE})_{\text{df}} = \exp\left\{T \int_{-1/2T}^{1/2T} \log\left(\frac{X_0(f)}{N_0} + 1\right)^{-1} \text{df}\right\}, \tag{49}$$

where

$$X_0(f) = \frac{1}{T}\sum_n \left|G_1\left(f + \frac{n}{T}\right) + jG_2\left(f + \frac{n}{T}\right)\right|^2 \times \left|C_1\left(f + \frac{n}{T}\right) + jC_2\left(f + \frac{n}{T}\right)\right|^2.$$

The passband transmitter and channel characteristics are denoted by $G_1 + jG_2$ and $C_1 + jC_2$, respectively. For comparison purposes, it is simple to show that the matched filter bound is

$$(\text{MMSE})_{\text{mf}} = \left\{T \int_{-1/2T}^{1/2T} \left(\frac{X_0(f)}{N_0} + 1\right)\text{df}\right\}^{-1}. \tag{50}$$

It is of interest to note that we can prove that expressions (48), (49), and (50) follow the sequence

$$(48) \leqq (49) \leqq (50)$$

by invoking Jensen's Inequality for the logarithm as the concave function. It is clear that, for the ideal channel and transmitter, i.e., $X_0(f) \equiv 1/T$, we have

$$(\text{MMSE})_{\text{linear}} = (\text{MMSE})_{\text{df}} = (\text{MMSE})_{\text{mf}} = \frac{1}{1 + (N_0T)^{-1}}.$$

APPENDIX D

A technique for separating transmitter and receiver filters

We wish to determine that factorization of

$$A(z^{-1})B(z^{-1}) = \prod_{n=0}^{N} Q_n(z^{-1}),$$

which minimizes $\|A(z^{-1})\|$ while $\|B(z^{-1})\| = 1$. Each

$$Q_n(z^{-1}) = 1 + a_1^{(n)}z^{-1} + a_2^{(n)}z^{-2}$$

is a quadratic factor. We assume no real roots occur, although the extension of the technique we present here to include real roots is obvious. Now

$$\|Q_n(z^{-1})\|^2 = \int_{-\frac{1}{2}}^{\frac{1}{2}} |Q_n(e^{-j2\pi fT})|^2 df = 1 + (a_1^{(n)})^2 + (a_2^{(n)})^2.$$

We notice that, upon choosing $B(z^{-1}) = \prod_{n_k \in N_B} Q_{n_k}(z^{-1})$ (where $N_B \cup N_A = \{0, 1, 2, \cdots, N\}$), then

$$\|A(z^{-1})\| = \|\prod_{n_k \in N_B} Q_{n_k}(z^{-1})\| \, \|\prod_{n_m \in N_A} Q_{n_m}(z^{-1})\|. \tag{51}$$

Thus, what we really want to do is select a partition of the Q_k factors so that the product of the norms of the partition factors is minimized. Much like the quadratic factor partitioning problem in digital filter implementation for minimizing roundoff noise, the only method for obtaining the global minimum of $\|A(z^{-1})\|$ seems to be the formation of all possible combinations of quadratic factors. When N is large, say, 20, this combinatorial method is time-consuming even when the filters are forced to be of the same order.

A technique for constructing the partition which sequentially minimizes $\|A(z^{-1})\|$ is first begun by reordering the quadratic factors by norm $\{Q_{nl}\}_{l=0}^{N}$. We think of the two norms of (51) as bins, and we sequentially fill those bins with quadratic factors. We insert one of two quadratic factors of largest norms into the first bin and the second factor into that same bin. We evaluate the norm of the first bin and now compare it to the product of the norms of the individual factors. Whichever placement results in smaller norm product, we choose as our partition initialization. Thus, at the end of the first step we have either

$$\overset{\text{bin 1}}{\|Q_{n_1}Q_{n_2}\|} \quad \overset{\text{bin 2}}{\|1\|}$$

or

$$\overset{\text{bin 1}}{\|Q_{n_1}\|} \quad \overset{\text{bin 2}}{\|Q_{n_2}\|},$$

depending on which product is smaller. The next factor, Q_{n_3}, is brought into the current partition and the products again are tested as to whether Q_{n_3} minimizes the product when placed in bin 1 or bin 2. The process continues until all quadratic factors are placed into either bin.

This procedure has been programmed and tested on actual filter quadratic factors. It has been our experience that the resulting factorization was close to the optimal one. To cite an example: Ten quadratic factors were randomly placed into two bins 500 times. The product of the norms of the two bins' contents ranged from 0.584 to 1183.33. The partition which our procedure yields for this set of quadratic factors had the product value of 0.646. Only 36 of the 500 partitions yielded smaller products. But little could be gained by using any of these 36 partitions. However, the worst partition was four orders of magnitude away from the outcome of our procedure. This is possibly what is most important, namely finding a partition very far away from the worst one.

REFERENCES

1. J. Salz, "Optimum Mean Square Decision Feedback Equalization," B.S.T.J., *52*, No. 8 (October 1973), pp. 1341–1373.
2. D. D. Falconer and G. J. Foschini, "Theory of Minimum Mean Square Error QAM Systems Employing Decision Feedback Equalization," B.S.T.J., *52*, No. 9 (December 1973), pp. 1821–1849.
3. P. R. Halmos, *Introduction to Hilbert Space and the Theory of Spectral Multiplicity*, New York: Chelsea, 1957, p. 32.
4. T. W. Thatcher, Jr., and F. D. Duffy, "Analog Transmission Performance of Toll Connections on the DDD Telephone Network," B.S.T.J., *50*, No. 4 (April 1971), pp. 1311–1347.